Upward Needleless Electrospinning of Nanofibers

Haitao Niu, Ph.D., Xungai Wang, Ph.D., Tong Lin, Ph.D.

Deakin University, Geelong, Victoria AUSTRALIA

Correspondence to:
Tong Lin email: tong.lin@deakin.edu.au

ABSTRACT

Polyacrylonitrile (PAN) nanofibers were prepared by a needleless electrospinning method using three rotating fiber generators, cylinder, disc and coil. The effects of the spinneret shape on the electrospinning process and resultant fiber morphology were examined. The disc spinneret needed the lowest voltage to initiate fiber formation, followed by the coil and cylinder. Compared to cylinder, the disc and coil produced finer fibers with narrower diameter distribution. The productivity of a coil was 23 g/hr, which was much larger than that of the cylinder spinneret having the same length and diameter. Finite elementary method was used to analyze the electric field. Stronger electric field was found to be formed on disc and coil surface, which concentrated on the disc circumferential edge and coil wire surface, respectively. For cylinder, the high intensity electric field was mainly concentrated on the end area. Concentrated electric field on the fiber generating surface could be used to explain the better electrospinning performance of coil, which may form a new concept for designing needleless electrospinning spinnerets.

Keywords: Fiber generator; Mass production; Nanofibers; Needleless electrospinning; PAN.

ITRODUCTION

Electrospinning is a simple, but efficient and versatile technology to produce polymeric nanofibers for widely diverse applications. This technique has shown many advantages, such as universality in processing polymeric materials, eases of controlling the fiber diameter and functionalizing nanofibers through adding functional agents to the electrospinning solution, and flexibility to generate fibrous membranes with desired geometries. Electrospun nanofibers have enormous potential for applications in areas as diverse as filtration [1], tissue engineering [2, 3], sensors [4], energy conversion and storage [5-7], catalysis [8], and many others.

An electrospinning setup generally consists of a solution vessel, a fiber generator (also referred to as "Spinneret") connected with a high voltage power supply, a collector connected to an opposite polarity. In a conventional electrospinning setup, a needle-like spinneret is often used, which has a low fiber production rate. Efforts have been made to improve the electrospinning productivity by replacing the needle spinneret with other spinnerets, such as conical wire coil, plate, splashing spinneret, rotary cone, and bowl edge [9-13]. Although these spinnerets showed improvement in productivities, some external assistance, from magnetic field [14], or high pressure gas [15] is required.

Recently, a needleless setup using a rotary spinneret to upward electrospin nanofibers has shown considerable improvement in the nanofiber production rate. The earliest rotating electrospinning can be dated back to 1970s when Simm *et al* [16] filed a patent on using rings to electrostatically spin fibers. In 2005, Jirsak *et al* [17] patented a roller electrospinning, which has been commercialized by Elmarco with the brand name Nanospider™. Previously we have used cylinder and disc as fiber generators to perform needleless electrospinning and shown the effect of spinneret shape [18]. We also filed our coil electrospinning [19].

Despite of the success in needleless electrospinning, a design principle for developing better needleless electrospinning spinnerets is still lacking. In this paper, by using three rotating fiber generators, cylinder, disc and coil, we elucidate the influences of spinneret shape on electrospinning process, fiber diameter and productivity. PAN was used as a model polymer. The electric field generated by these spinnerets was also analyzed by a finite element method and the calculation results indicated that electric field intensities on these spinnerets distributed differently.

EXPERIMENTAL METHODS

Materials

Polyacrylonitrile (PAN, Sigma-Aldrich, Mw~ 150,000) and dimethylformamide (DMF) were obtained from Aldrich-Sigma and used as received. The PAN solution was prepared by dissolving PAN in DMF and stirring at 80 °C for 6 hours. A 9 wt% PAN solution was used throughout the experiment.

Electrospinning

The needleless electrospinning setup is schematically depicted in *Figure 1*, which comprises a rotary metal fiber generator, a Teflon solution vessel, a high voltage power supply (ES50P-20W/DAM, Gamma High Voltage Research), and a grounded rotating drum collector. Cylinder, disc, and spiral coil were used as fiber generators, their dimensions are listed in *Table I*. A high voltage was applied to the bottom of solution bath via a copper electrode. During electrospinning, the polymer solution was loaded onto the spinneret surface by the slow rotation (speed 40 rpm). The applied voltage and collecting distance were 60 kV and 13 cm, respectively. Electrospun PAN nanofibers were collected on the drum collector which was covered with stainless steel mesh.

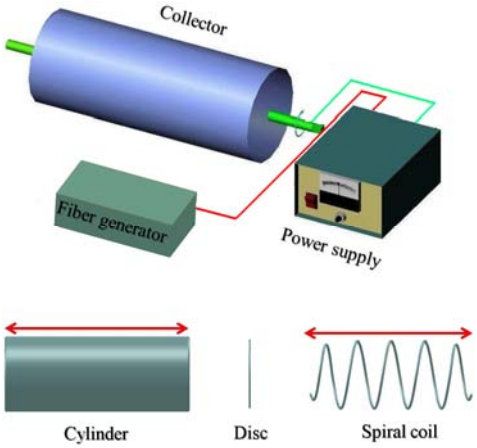

FIGURE 1. Schematic illustration of needless electrospinning and fiber generators.

Electric Field Analysis

The electric field was calculated by a finite element method, using a commercial program COMSOL3.5. The spinnerets, solution vessel, polymer solution, and collector were transformed into geometrical objects in COMSOL, and their practical dimensions, locations, and relative permittivity were input. The collector and infinite boundaries were set as zero potential. The rest boundaries were set as continuity. COMSOL performed the meshing and solving to obtain the electric field information.

Characterization

Scanning electron microscopy (SEM, Supra 55 VP) was used to observe the fiber morphology. The average fiber diameter was calculated using the software (Image*Pro*+6.0) based on the SEM images. The productivity of needleless electrospinning was measured based on the dry weight of collected nanofibers.

RESULTS AND DISCUSSION

Electric Field Analysis

It has been known that electric field is the driving force for needle electrospinning, which leads to the formation of "Taylor cone" and initiation of jet [20]. In needleless electrospinning, solution jets were generated from an open solution surface. This made the jet initiation process quite different from that in needle electrospinning.

The electric field intensity profiles of three fiber generators were calculated with applied voltage of 60 kV. As illustrated in *Figure 2* the electric field intensity on different area of the same spinneret varied. The high intensity electric field was mainly formed on the cylinder ends and much lower intensity electric field was formed on the cylinder middle surface area. However, for disc spinneret, high intensity electric field was mainly formed at the circumferential edge, and the intensity value was higher than that on the cylinder. It was interesting to note that all the coil top surface area where nanofibers were generated had high electric field intensity. Due to the interference between adjacent spirals, the spirals close to coil ends formed electric field with the higher intensity.

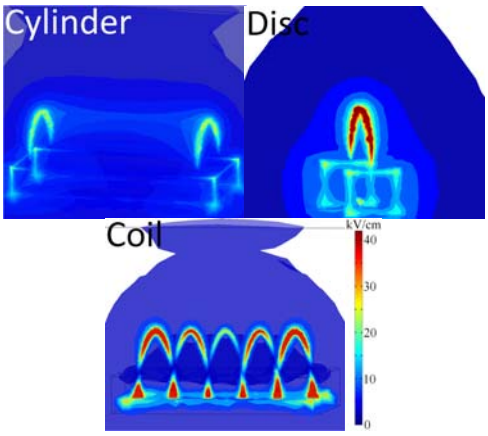

FIGURE 2. Electric field intensity profiles of cylinder, disc, and spiral coil spinnerets.

Figure 3 shows the electric field intensity from the spinneret surface to the collector. The intensity at the spinneret surface was the highest, and it decayed

rapidly away from the spinneret to the collector. The electric field gradient has been previously reported to be helpful to the jet initiation on the spinneret surface [10, 22]. Therefore, the disc and coil spinnerets, forming electric field with higher electric field gradients, will facilitate the jet initiation. On the cylinder end, the electric field intensity was 22 kV/cm, while electric field with much lower intensity 9 kV/cm was formed at the cylinder middle area. Disc spinneret formed stronger electric field (65 kV/cm) at the circumferential edge compared to the cylinder. Due to the interference between spirals, the electric field formed on the spirals had three different intensities 25 kV/cm, 38 kV/cm, 64 kV/cm respectively. The electric field on end spiral surface had nearly the same intensity with that of disc.

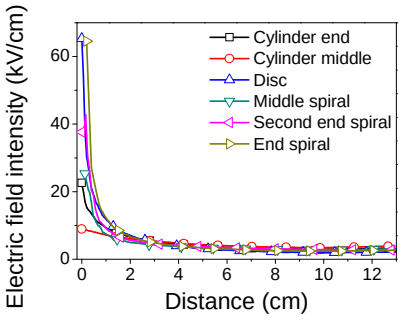

FIGURE 3. Electric field intensity from the spinneret surface to collector.

The electric field intensity along the spinneret axis direction is shown in *Figure 4*. For cylinder spinneret, electric field at the end area was stronger but it decayed and then stabilized toward the cylinder middle area. The five spirals in the coil spinneret formed electric field with five strength peaks on the surface. The electric field intensity profile of each spiral was similar to that formed by a disc spinneret but with lower intensity value. It can be concluded that the coil spinneret possessed the features from both the cylinder and the disc spinnerets, by forming narrowly distributed electric field on the wire surface.

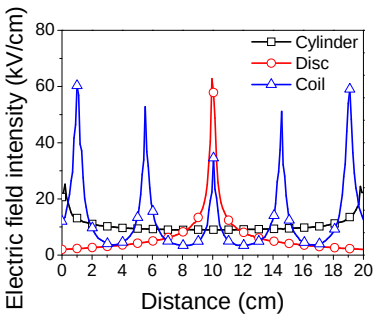

FIGURE 4. Electric field intensity at the spinneret top along the axis direction (indicated as the double-headed arrow in *Figure 1*).

Electrospinning Process

The critical voltage to initiate electrospinning process varied between the three different setups. As listed in *Table I*, fibers can only be generated on cylinder end area when the applied voltage was over 47 kV. Only when the applied voltage was higher than 57 kV can the middle surface generate nanofibers. In comparison, the critical voltages to initiate nanofibers on disc and spiral coil were lower, 42 kV and 45 kV respectively.

TABLE. I. Dimension of spinnerets and critical voltages.

	Dimension (mm)	Critical Voltage (kV)
Cylinder	Φ = 80 L = 200	47 (two top ends); 57kV (top ends + top middle)
Disc	Φ = 80 D = 2	42 (top disc edge)
Spiral Coil	Φ = 80 L = 200	45 (top coil)

Φ: Diameter of fiber generator; L: Cylinder and spiral coil length; D: Disc thickness

Lukas *et al* [21] have developed a one-dimensional electrohydrodynamic theory to describe the electrospinning of conductive liquids from an open flat surface based on the phenomenon that nanofibers can be electrospun from linear clefts. They pointed out that the fastest growing stationary wave led to the onset of electrospinning from a free liquid surface with its jets originated from the wave crests.

The jet initiating in needleless electrospinning may follow a few different stages: 1) formation of a thin solution layer on the spinneret surface, 2) initiation of conical spikes on the solution surface due to the rotation of spinneret and gravity effect, 3) concentration of electric force on the spikes, and the formation of "Taylor cone" as a consequence, and 4) jets formation.

Figure 5 shows electrospinning process of the three setups. Numerous PAN nanofibers were generated from the spinnerets, when the applied voltage was 60 kV. For cylinder, the fiber generating area covered both the end and middle area. However, more dense jets were formed from the small area of disc circumferential edge and coil wires. The solution jets moved along with the rotating spinneret until the spinneret surface re-entered the solution bath. Electrospun nanofibers solidified and were deposited onto the collector above.

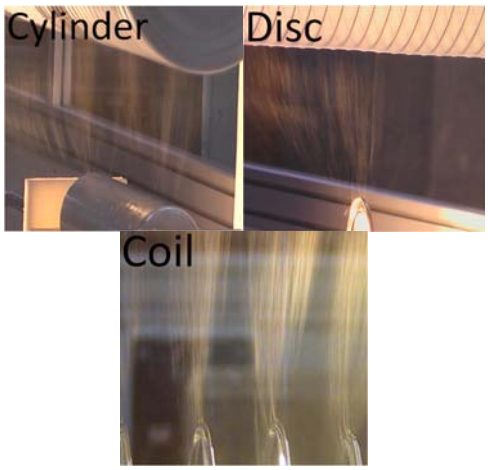

FIGURE 5. Photos of needleless electrospinning processes.

Fiber Production Rate and Property

Figure 6 shows the morphology of PAN nanofibers electrospun from different spinnerets. All these nanofibers exhibited uniform fibrous structure.

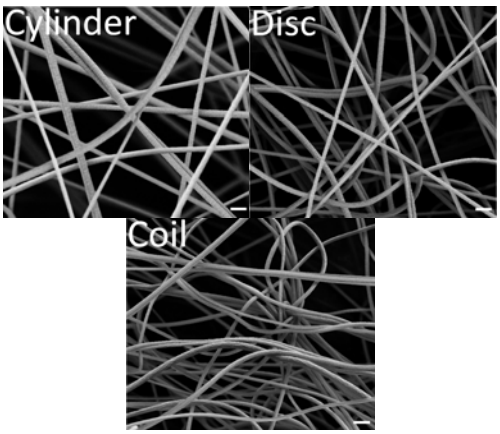

FIGURE 6. SEM images of PAN nanofibers electrospun by cylinder, disk, and spiral coil spinnerets (scale bar = 1 μm).

As shown *Figure 7*, nanofibers produced by the disc spinneret were finer with narrower diameter distribution (better quality). A thin disc (diameter 8 cm and thickness 2 mm) could produce nanofibers at a similar rate to a cylinder of the same diameter but 100 times wider (i.e. 20 cm long). However, the coil that has the same length and diameter to the cylinder was double in the production rate, and the produced fibers were finer with narrower diameter distribution.

For comparison, needle electrospinning was also performed. Nanofibers electrospun by needle nozzle had larger fiber diameter. For the disc and coil systems, attributed to their narrowly distributed electric field overlapping the fiber generating area, they produced even finer nanofibers than the conventional electrospinning system.

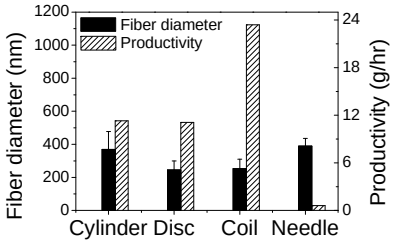

FIGURE 7. Fiber diameters of electrospun PAN nanofibers and productivities.

Electric field analysis can be used to understand the electrospinning behaviors. For cylinder, electrospinning takes place in both areas that the one has high electric field intensity and the other has low. Fibers produced from the two areas should have a large difference in fiber diameter. As a result, the fibers in average would have a large diameter and diameter distribution. For disc and coil spinnerets, the fibers are mainly generated from the area that has high electric field intensity. This not only produces finer fibers but also narrows the diameter distribution. The spiral coil has multiple fiber-generating areas with high electric field intensity. This makes it have a much larger production rate than disc.

The X-ray diffraction result of PAN nanofibers electrospun by needle and needleless electrospinning is shown in *Figure 8*. Both curves contain two diffraction peaks at 17° and 29°, corresponding to the (10) and (11) reflections respectively [23, 24]. The peak at 17° in the needleless electrospun nanofibers was stronger and shaper than that of nanofibers produced by conventional needle electrospinning, indicating higher PAN crystallinity within the needleless electrospun nanofibers. The higher polymer crystallinity could facilitate with improving the fiber mechanical strength.

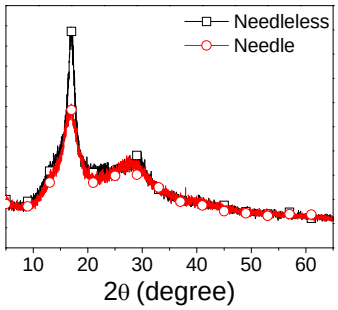

FIGURE 8. XRD patterns of needle and needleless electrospun nanofibers.

CONCLUSION

We have used cylinder, disc, and spiral coil as fiber generators to perform needleless electrospinning. The results revealed that fiber generator geometry had considerable influences on the electric field intensity and profiles, which ultimately affected the electrospinning process, the fiber diameter and productivity. The electric field analysis indicated that high electric field intensity was formed by disc and coil spinnerets, which distributed narrowly on the surface of disc circumferential edge and coil wire respectively. The cylinder spinneret formed unevenly distributed electric field at the end and middle area with lower strength. The intensity peak was formed only on the coil surface. Finer nanofibers with narrower diameter distribution were produced by disc and coil spinnerets, compared to needle and cylinder electrospinning. The fiber production rate in coil electrospinning was as high as 23 g/hr, which was much higher than those in cylinder, disc, and needle electrospinning. PAN nanofibers produced by needleless electrospinning showed improved crystallinity compared to those from needle electrospinning. All these results indicate that an electrospinning fiber generator that can generate narrowly distributed electric field overlapping the fiber generating area will facilitate the mass production of high quality nanofibers in needleless electrospinning fashion.

REFERENCES

[1] Gopal, R., Kaur, S., Ma, Z., et al., Electrospun nanofibrous filtration membrane, *Journal of Membrane Science*, 281, 2006, 581.

[2] Yoshimoto, H., Shin, Y. M., Terai, H., et al., A biodegradable nanofiber scaffold by electrospinning and its potential for bone tissue engineering, *Biomaterials*, 24, 2003, 2077.

[3] Desai, K., Kit, K., Li, J., et al., Nanofibrous chitosan non-wovens for filtration applications, *Polymer*, 50, 2009, 3661.

[4] Wang, X., Drew, C., Lee, S. H., et al., Electrospun Nanofibrous Membranes for Highly Sensitive Optical Sensors, *Nano Letters*, 2, 2002, 1273.

[5] Kim, C., Yang, K. S., Kojima, M., et al., Fabrication of electrospinning-derived carbon nanofiber webs for the anode material of lithium-ion secondary batteries, *Advanced Functional Materials*, 16, 2006, 2393.

[6] Prilutsky, S., Schechner, P., Bubis, E., et al., Anodes for glucose fuel cells based on carbonized nanofibers with embedded carbon nanotubes, *Electrochimica Acta*, 55, 2010, 3694.

[7] Kim, C., Choi, Y. O., Lee, W. J., et al., Supercapacitor performances of activated carbon fiber webs prepared by electrospinning of PMDA-ODA poly(amic acid) solutions, *Electrochimica Acta*, 50, 2004, 883.

[8] Jia, H., Zhu, G., Vugrinovich, B., et al., Enzyme-Carrying Polymeric Nanofibers Prepared via Electrospinning for Use as Unique Biocatalysts, *Biotechnology Progress*, 18, 2002, 1027.

[9] Wang, X., Niu, H., Lin, T., et al., Needleless electrospinning of nanofibers with a conical wire coil, *Polymer Engineering & Science*, 49, 2009, 1582.

[10] Thoppey, N. M., Bochinski, J. R., Clarke, L. I., et al., Unconfined fluid electrospun into high quality nanofibers from a plate edge, *Polymer*, 51, 2010, 4928.

[11] Tang, S., Zeng, Y., Wang, X., Splashing needleless electrospinning of nanofibers, *Polymer Engineering & Science*, 50, 2010, 2252.

[12] Lu, B., Wang, Y., Liu, Y., et al., Superhigh-Throughput Needleless Electrospinning Using a Rotary Cone as Spinneret, *Small*, 6, 2010, 1612.

[13] Thoppey, N. M., et al., Edge electrospinning for high throughput production of quality nanofibers, *Nanotechnology*, 22, 2011, 345301.

[14] Yarin, A. L., Zussman, E., Upward needleless electrospinning of multiple nanofibers, *Polymer*, 45, 2004, 2977.

[15] Liu, Y., He, J.-H., Yu, J.-Y., Bubble-electrospinning: a novel method for making nanofibers, *Journal of Physics: Conference Series*, 96, 2008, 012001.

[16] Simm, W., Gosling, C., Bonart, R., et al., United States pat. 1979).

[17] JIRSAK, O., SANETRNIK, F., LUKAS, D., et al., A method of nanofibres production from a polymer solution using electrostatic spinning and a device for carrying out the method, *WO 2005/024101 A1*, 2005.

[18] Niu, H., Lin, T., Wang, X., Needleless electrospinning. I. A comparison of cylinder and disk nozzles, *Journal of Applied Polymer Science*, 114, 2009, 3524.

[19] Lin, T., Wang, X., Wang, X., et al., Electrostatic spinning assembly, *WO/2010/043002*, 2010,
[20] Taylor, G., Electrically driven jets, *Proceedings of the Royal Society of London. Series A, Mathematical and Physical Sciences*, 313, 1969, 453.
[21] Lukas, D., Sarkar, A., Pokorny, P., Self-organization of jets in electrospinning from free liquid surface: A generalized approach, *Journal of Applied Physics*, 103, 2008, 084309.
[22] Yang, Y., Jia, Z., Liu, J., et al., Effect of electric field distribution uniformity on electrospinning, *Journal of Applied Physics*, 103, 200 8, 104307.
[23] Fennessey, S. F., Farris, R. J., Fabrication of aligned and molecularly oriented electrospun polyacrylonitrile nanofibers and the mechanical behavior of their twisted yarns, *Polymer*, 45, 2004, 4217.
[24] Davidson, J. A., Jung, H. T., Hudson, S. D., et al., Investigation of molecular orientation in melt-spun high acrylonitrile fibers, *Polymer*, 41, 2000, 3357.

AUTHORS' ADDRESSES

Haitao Niu, Ph.D.
Xungai Wang, Ph.D.
Tong Lin, Ph.D.
Deakin University
Pigdons Rd
Geelong, Victoria 3216
AUSTRALIA